AIAA 79-1672R

Closed-Form Solution for Ballistic Vehicle Motion

Frank J. Barbera*
Kaman Sciences Corporation, Colorado Springs, Colo.

A closed-form solution is developed for the motion of a ballistic vehicle entering the atmosphere over a flat nonrotating Earth. The Allen and Eggers approach of using an exponential atmosphere is retained; however, the vehicle drag coefficient is expressed as a function of velocity instead of being considered a constant. Use of the derived equations allows an analyst to solve directly for the vehicle velocity at any point along the trajectory, as well as for the maximum axial acceleration and the altitude at which it occurs.

Nomenclature

A = aerodynamic reference area
a_x = axial acceleration, g
a, a_1, a_2 = constants in the drag coefficient relation [see Eq. (16)]
C_D = aerodynamic drag coefficient
C_1 = $e^{-\eta_1 y_\rho}$
C_2 = $e^{-\eta_2 y_\rho}$
C_3 = $C_1\lambda_1 - C_2\lambda_1'$
C_4 = $C_1\lambda_2 - C_2\lambda_2'$
C_5 = $V_B^{-m_2} + (\xi_2/\xi_1)(V_E^{-m_1} - V_B^{-m_1})$
M = Mach number
m, m_1, m_2 = constants in the drag coefficient relation [see Eq. (16)]
q_∞ = dynamic pressure = $\frac{1}{2}\rho_\infty V^2$
R_B = vehicle base radius
R_N = vehicle nose radius
t = time
V = velocity
V_B = break point velocity (see Fig. 3)
V_ρ = velocity at y_ρ
W = vehicle weight
x, y = horizontal and vertical distance from the point of impact with the Earth
Y_{B1}, y_{B2} = altitude where the break velocity is reached [see Eqs. (23) and (24)]
Y_ρ = altitude where the slope of the atmospheric density function changes
β, β_{hyp} = vehicle ballistic coefficient defined by Eq. (3) [see Eq. (17)]
ξ, ξ_1, ξ_2 = $am, a_1 m_1, a_2 m_2$
η, η_1, η_2 = constants in the density-altitude relation [see Eq. (7) and Fig. 2]
γ = angle between the flight path and the horizontal (see Fig. 1)
θ_c = cone half-angle
λ = $\xi\phi'/\eta$
λ_1, λ_2 = $\xi_1\phi_2'/\eta_1, \xi_2\phi_1'/\eta_1$
λ_1', λ_2' = $\xi_1\phi_2'/\eta_2, \xi_2\phi_2'/\eta_2$
ρ = mass density of the air
ρ_{01}, ρ_{02} = constants in the density-altitude relation (see Fig. 2)
ϕ, ϕ' = constants defined by Eq. (9) [see Eq. (19)]
ϕ_1', ϕ_2' = constants defined by Eq. (22)

Superscripts

( )* = values at the time of maximum axial acceleration

Subscripts

0 = initial conditions
B = drag coefficient slope change point
E = value at the re-entry altitude
I = value at impact
hyp = hypersonic value
ρ = atmospheric density slope change point
∞ = freestream value

Introduction

THE closed-form solution to ballistic vehicle motion described by Allen and Eggers[1] has been exceptionally useful to re-entry vehicle analysts for years because the solution points out the important variables of the problem and how they interact. Their assumption of an exponential atmosphere and the neglect of the gravity term in the equations of motion have been shown to be very reasonable approximations, and they will be utilized in the present derivations as well. Their use of a constant drag coefficient, although very reasonable for many applications, has been too restrictive for some purposes.

The present paper introduces an integrable expression for the vehicle drag coefficient that is a function of the velocity. The Mach number dependent inviscid drag coefficients of typical re-entry vehicles have been closely matched using the velocity expression. The resulting relations for the equations of motion have been solved in closed form. The analytical equations which result are very simple, and an analyst can evaluate the important variables of a re-entry trajectory with reasonable accuracy using a hand calculator.

Analysis

Equations of Motion

Consider a re-entry vehicle entering the atmosphere over a flat nonrotating Earth, with the coordinate system defined in Fig. 1. The equations of motion can be written as

$$\frac{d^2y}{dt^2} = -g + \frac{\rho g V^2}{2\beta}\sin\gamma \tag{1}$$

and

$$\frac{d^2x}{dt^2} = \frac{\rho g V^2}{2\beta}\cos\gamma \tag{2}$$

where β is the ballistic coefficient of the vehicle defined by

$$\beta = W/C_D A \tag{3}$$

Presented as Paper 79-1672 at the AIAA Atmospheric Flight Mechanics Conference, Boulder, Colo., Aug. 6-8, 1979; submitted Oct. 19, 1979; revision received May 1, 1980.

*Manager, Aerothermal Support Group. Member AIAA.

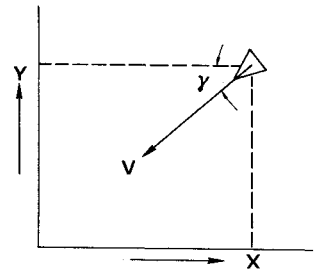

Fig. 1 Coordinte system.

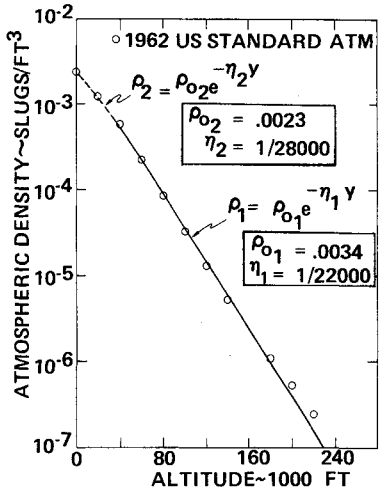

Fig. 2 Variation of density with altitude.

It has been demonstrated by Allen and Eggers[1] that when the vehicle enters the atmosphere at high speed, and when the angle γ_E is not too small, then the gravity term may be neglected in Eq. (1) to yield

$$\frac{d^2y}{dt^2} = \frac{\rho g V^2}{2\beta} \sin\gamma \tag{4}$$

With this assumption, the flight path is essentially a straight line (i.e., $Y = Y_E$) and the resultant deceleration equation becomes

$$\frac{dV}{dt} = -\frac{\rho g V^2}{2\beta} \tag{5}$$

Note that $dy/dt = -V\sin\gamma_E$, and from calculus, $dV/dt = (dy/dt)\,(dV/dy)$, thus

$$\frac{dV}{dt} = -V\sin\gamma_E \frac{dV}{dy} \tag{6}$$

Assuming an exponential atmosphere, such as illustrated in Fig. 2, the relation

$$\rho = \rho_0 e^{-\eta y} \tag{7}$$

can be used with Eqs. (4) and (5) to yield

$$\frac{dV}{V} = -\phi e^{-\eta y} dy \tag{8}$$

where ϕ is defined as

$$\phi = -g\rho_0/2\beta\sin\gamma_E \tag{9}$$

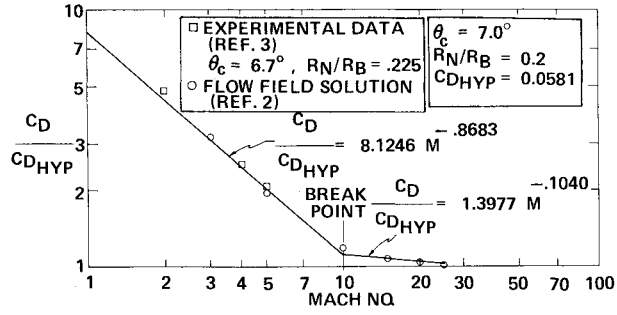

Fig. 3 Normalized drag coefficient vs Mach number.

Constant Drag Coefficient Relations

If the drag coefficient in Eq. (3) is assumed constant, and if a single function is used to characterize the atmospheric density over the entire altitude range, then the relations derived in Ref. 1 are obtained by integrating Eq. (8). The results will be repeated here for completeness. The trajectory velocity is given by

$$V = V_E \exp(\phi/\eta) e^{-\eta y} \tag{10}$$

and the axial acceleration (in g) is

$$a_x = (\phi\sin\gamma_E/g)\, V_E^2 e^{-\eta y} \exp(2\phi/\eta) e^{-\eta y} \tag{11}$$

The altitude at which the maximum deceleration occurs is found from this relation to be

$$y^* = (1/\eta)\ln(-2\phi/\eta) \tag{12}$$

If y^* occurs prior to impact ($y^* > 0$), then the velocity at which the maximum acceleration occurs is

$$V^* = V_E e^{-1/2} \approx 0.61\ V_E \tag{13}$$

and the value of the maximum acceleration (in g) is

$$a_x^* = \eta V_E^2 \sin\gamma_E / 2ge \tag{14}$$

If y^* is negative, then the maximum deceleration occurs at sea level. The time to any altitude was not treated in Ref. 1, but it was derived by the present author in the form of the following series solution:

$$t = \frac{1}{V_E \eta \sin\gamma_E}\left[\eta(y_E - y) - \left(\frac{\phi}{\eta}\right)e^{-\eta y} + \frac{1}{4}\left(\frac{\phi}{\eta}\right)^2 e^{-2\eta y} - \frac{1}{18}\left(\frac{\phi}{\eta}\right)^3 e^{-3\eta y} + \frac{1}{96}\left(\frac{\phi}{\eta}\right)^4 e^{-4\eta y} + \frac{1}{600}\left(\frac{\phi}{\eta}\right)^5 e^{-5\eta y} + \ldots\right] \tag{15}$$

where six terms must be used to achieve accuracy to a millisecond.

Velocity Dependent Drag Coefficient

When the Mach number dependent inviscid drag coefficient of a sphere-cone re-entry vehicle is normalized by its hypersonic value and then plotted on log-log paper, it characteristically exhibits two straight line segments, such as illustrated in Fig. 3. If it is assumed that the speed of sound is a constant over the altitude range of interest, then with small error one can model the vehicle inviscid drag coefficient as a function of velocity using the relation

$$C_D/C_{D_{\text{hyp}}} = aV^m \tag{16}$$

Table 1 Drag coefficient parameters

	R_N/R_B					
θ_c, deg	0.0	0.1	0.2	0.3	0.4	
6	23.130	14.867	3.043	2.210	1.573	a_1
7	13.527	9.485	2.867	2.046	1.590	
8	8.404	5.610	3.861	2.246	1.590	
6	51,927	33,219	2466	564	80	a_2
7	17,345	14,912	3271	520	71	
8	7,565	5,334	1564	322	73	
6	−0.3102	−0.2666	−0.1099	−0.0783	−0.0447	m_1
7	−0.2572	−0.2222	−0.1040	−0.0707	−0.0458	
8	−0.2102	−0.1703	−0.1334	−0.0799	−0.0458	
6	−1.1394	−1.0912	−0.8332	−0.7003	−0.4897	m_2
7	−1.0301	−1.0131	−0.8683	−0.6920	−0.4742	
8	−0.9449	−0.9072	−0.7853	−0.6357	−0.4784	
6	11,000	11,500	10,500	7,400	6,800	V_B
7	10,500	1,000	10,000	7,400	7,000	
8	10,500	11,000	10,000	7,600	7,000	
6	0.0246	0.0276	0.0531	0.1001	0.1644	$C_{D_{hyp}}$
7	0.0326	0.0352	0.0581	0.1052	0.1699	
8	0.0418	0.0444	0.0635	0.1101	0.1745	

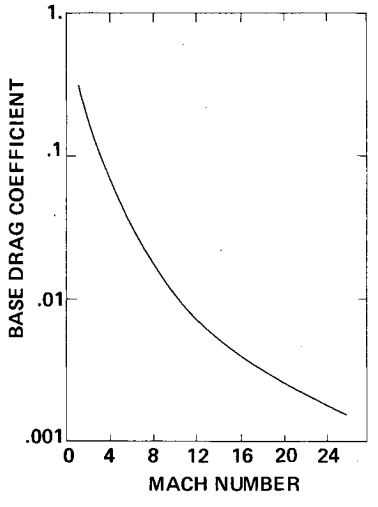

Fig. 4 Base drag coefficient vs Mach number.

where a_1 and m_1 are the values of the constants in the hypersonic Mach number region, and a_2 and m_2 are the values of the constants in the supersonic Mach number region. $C_{D_{hyp}}$ is the value of the inviscid drag coefficient as $m \to \infty$, and for a given vehicle configuration, $C_{D_{hyp}} = \text{constant}$.

Some typical re-entry vehicles were analyzed, using the Moretti flowfield code,[2] to obtain the inviscid, perfect gas, wave drag coefficient. The base drag variation shown in Fig. 4 was then added to the wave drag, for each configuration analyzed, and the resultant total inviscid drag variation was curve fit using Eq. (16). The resulting constants are presented in Table 1 for vehicles with various combinations of the cone half-angle and the bluntness ratio R_N/R_B.

Variable Drag Coefficient Relations

If C_D in Eq. (3) is replaced with the variable drag coefficient relation of Eq. (16), and if a hypersonic ballistic coefficient is defined as

$$\beta_{hyp} = W/C_{D_{hyp}} A = \text{const} \tag{17}$$

then the following revised form of Eq. (8) is obtained:

$$\frac{dV}{V^{m+1}} = -a\phi' e^{-\eta y} dy \tag{18}$$

where

$$\phi' = -g\rho_0/2\beta_{hyp}\sin\gamma_E = \text{const} \tag{19}$$

Equation (18) can be integrated to yield the following expression for the trajectory velocity:

$$V = [\,V_0^{-m} - \lambda(e^{-\eta y} - e^{-\eta y_0})\,]^{-1/m} \tag{20}$$

where V_0 is the velocity at the initial altitude y_0.

When the re-entry vehicle first enters the atmosphere, $V_0 = V_E$ and $y_0 \approx 400{,}000$ ft. Under these conditions, Eq. (20) simplifies to

$$V = (\,V_E^{-m} - \lambda e^{-\eta y}\,)^{-1/m} \tag{21}$$

An attempt was made to solve for the time to any altitude using the differential equation $dy/dt = -V\sin\gamma_E$ and Eq. (20). The resulting time equation is

$$t = -\frac{1}{\sin\gamma_E}\int_{y_E}^{y} [\,V_E^{-m} - \lambda e^{-\eta y}\,]^{1/m} dy$$

which looks deceptively simple. Unfortunately, the solution was not obtained, which leaves one of the major parameters of a trajectory unsolved for the variable drag coefficient analysis.

In the remaining development, the atmospheric density variation with altitude is represented by two functions (see Fig. 2). One function is utilized above y_ρ, and the other function is utilized below y_ρ. The following new constants are required:

$$\phi_1' = \frac{-g\rho_{0_1}}{2\beta_{hyp}\sin\gamma_E} \qquad \phi_2' = \frac{-g\rho_{0_2}}{2\beta_{hyp}\sin\gamma_E} \tag{22}$$

When the re-entry velocity is greater than the break velocity, the hypersonic constants a_1 and m_1 must be used for the initial part of the trajectory. They can be used until the trajectory velocity decreases below V_B. Substitute V_B for V in Eq. (2) and solve for the altitude at which V_B is reached. For $y > y_\rho$,

$$Y_{B1} = \frac{1}{\eta_1}\ln\left(\frac{\lambda_1}{V_E^{-m_1} - V_B^{-m_1}}\right) \tag{23}$$

and when $y<y_\rho$,

$$Y_{B2}=\frac{1}{\eta_2}\ell n\left(\frac{\lambda_1'}{V_E^{-m_1}-V_B^{-m_1}-C_3}\right) \tag{24}$$

The break altitude for a re-entry vehicle having $\theta_c=7$ deg and $R_N/R_B=0.2$ is presented in Fig. 5 as a function of re-entry velocity. The figure is divided into four zones, where the velocity is either greater or less than the break velocity, and where the altitude is either greater or less than y_ρ (40,000 ft in this case). Different analytical expressions will be necessary in each zone.

Zone I Relations

The relations for determining the velocity and the axial acceleration (in g) as a function of altitude are given here for zone I, where $V>V_B$ and $y>y_\rho$:

$$V_1=(V_E^{-m_1}-\lambda_1 e^{-\eta_1 y})^{-1/m_1} \tag{25}$$

and

$$a_{x1}=e^{-\eta_1 y}V_1^{2+m_1}(a_1\phi_1\sin\gamma_e/g) \tag{26}$$

The altitude of maximum acceleration may or may not occur in a given zone, depending upon the conditions being investigated. The equations appropriate to zone I will be presented here, but the reader must determine which zone is appropriate for the conditions under consideration. This can usually be done by first solving for the altitude of maximum acceleration using the zone I relations. After noting which zone this altitude falls into, the appropriate equations can be used to obtain valid results.

For zone I, the altitude of maximum acceleration can be calculated using

$$Y_1^*=\frac{1}{\eta_1}\ell n\left(\frac{-2\lambda_1}{m_1 V_E^{-m_1}}\right) \tag{27}$$

The maximum acceleration (in g) is given by

$$a_{x1}^*=\frac{-V_E^2\eta_1\sin\gamma_E}{2g}\left(\frac{2+m_1}{2}\right)^{-(2+m_1)/m_1} \tag{28}$$

and the velocity at the altitude of maximum acceleration is

$$V_1^*=V_E[(2+m_1)/2]^{-1/m_1} \tag{29}$$

Zone II Relations

The following relations for zone II, where $V>V_B$ and $y<y_\rho$, are derived from Eq. (20) with $V_0=V_\rho$ and $y_0=y_\rho$:

$$V_2=(V_E^{-m_1}-C_3-\lambda_1' e^{-\eta_2 y})^{-1/m_1} \tag{30}$$

and

$$a_{x2}=e^{-\eta_2 y}V_2^{2+m_1}(a_1\phi_2\sin\gamma_E/g) \tag{31}$$

When the re-entry velocity is sufficiently large, then impact can occur in zone II (see Fig. 5). Solving for the re-entry velocity, which will cause the break velocity to occur at sea [using Eq. (24)], yields

$$(V_E)_{\lim}=[V_B^{-m_1}+C_3+\lambda_1']^{-1/m_1} \tag{32}$$

When $V_E\geq(V_E)_{\lim}$, then the impact occurs in zone II, and the following relation for impact velocity applies:

$$V_{I2}=[V_E^{-m_1}-(\lambda_1'+C_3)]^{-1/m_1} \tag{33}$$

The altitude of maximum axial acceleration in zone II is given by

$$Y_2^*=\frac{1}{\eta_2}\ell n\left[\frac{-2\lambda_1'}{m_1}\left(\frac{1}{V_E^{-m_1}-C_3}\right)\right] \tag{34}$$

The maximum axial acceleration (in g) is found using

$$a_{x2}^*=\left(\frac{-\eta_2\sin\gamma_E}{2g}\right)(V_E^{-m_1}-C_3)\times\left[\left(\frac{2+m_1}{2}\right)(V_E^{-m_1}-C_3)\right]^{-(2+m_1)/m_1} \tag{35}$$

and the velocity at maximum acceleration is

$$V_2^*=[(2+m_1)/2\cdot(V_E^{-m_1}-C_3)]^{-1/m_1} \tag{36}$$

Zone III Relations

The relations for zone III, where $V<V_B$ and $y<y_\rho$, are derived from Eq. (20) with $V_0=V_B$ and $y_0=y_B$:

$$V_3=(C_5-C_4-\lambda_2' e^{-\eta_2 y})^{-1/m_2} \tag{37}$$

and

$$a_{x3}=e^{-\eta_2 y}V_3^{2+m_2}(a_2\phi_2\sin\gamma_E/g) \tag{38}$$

The altitude of maximum axial acceleration in zone III is given by

$$Y_3^*=\frac{1}{\eta_2}\ell n\left[\frac{-2\lambda_2'}{m_2}\left(\frac{1}{C_5-C_4}\right)\right] \tag{39}$$

The maximum axial acceleration (in g) is found using

$$a_{x3}^*=\left(\frac{-\eta_2\sin\gamma_E}{2g}\right)(C_5-C_4)\left[\left(\frac{2+m_2}{2}\right)(C_5-C_4)\right]^{-(2+m_2)/m_2} \tag{40}$$

and the velocity at maximum acceleration is

$$V_3^*=\left[\left(\frac{2+m_2}{2}\right)(C_5-C_4)\right]^{-1/m_2} \tag{41}$$

In zone III, $V_E<(V_E)_{\lim}$, and the impact velocity is given by

$$V_{I3}=[(C_5-C_4)-\lambda_2']^{-1/m_2} \tag{42}$$

Zone IV Relations

The relations for zone IV, where $V<V_B$ and $y>y_\rho$, are derived from Eq. (20) with $V_0=V_E$ and $y_0=y_E$:

$$V_4(C_5-\lambda_2 e^{-\eta_1 y})^{-1/m_2} \tag{43}$$

and

$$a_{x4}=e^{-\eta_1 y}V_4^{2+m_2}(a_2\phi_1\sin\gamma_E/g) \tag{44}$$

The altitude of maximum axial acceleration in zone IV is given by

$$y_4^*=(1/\eta_1)\ell n(-2\lambda_2/m_2C_5) \tag{45}$$

The maximum acceleration (in g) is found using

$$a_{x4}^*=\frac{C_5^{-2/m_2}\eta_1\sin\gamma_E}{2g}\left(\frac{2+m_2}{2}\right)^{-(2+m_2)/m_2} \tag{46}$$

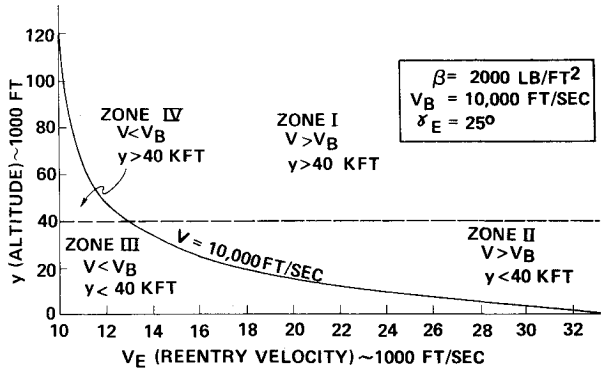

Fig. 5 Zones of applicability of the analytical relations.

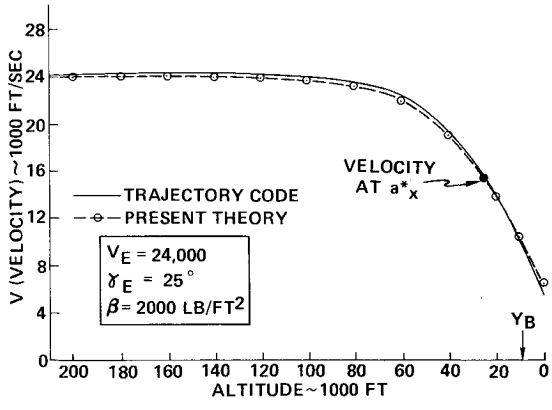

Fig. 6 Velocity vs altitude.

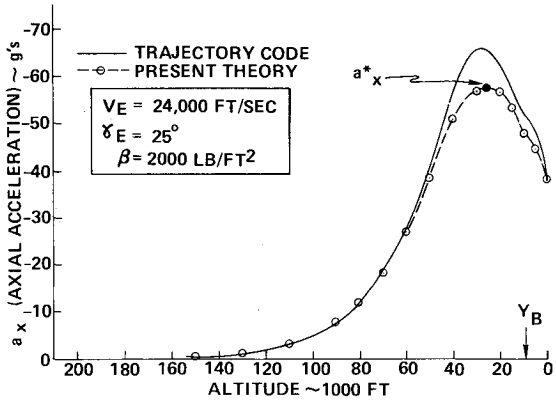

Fig. 7 Axial acceleration vs altitude.

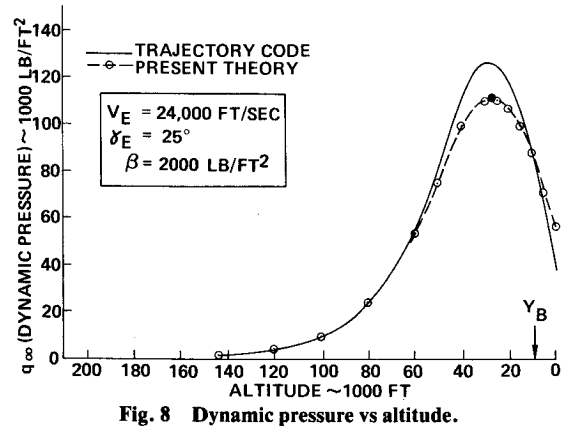

Fig. 8 Dynamic pressure vs altitude.

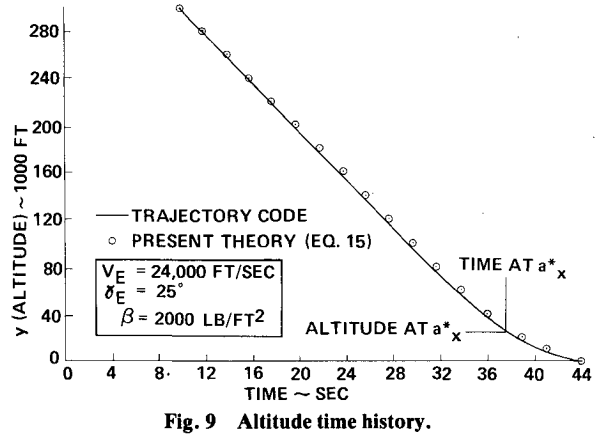

Fig. 9 Altitude time history.

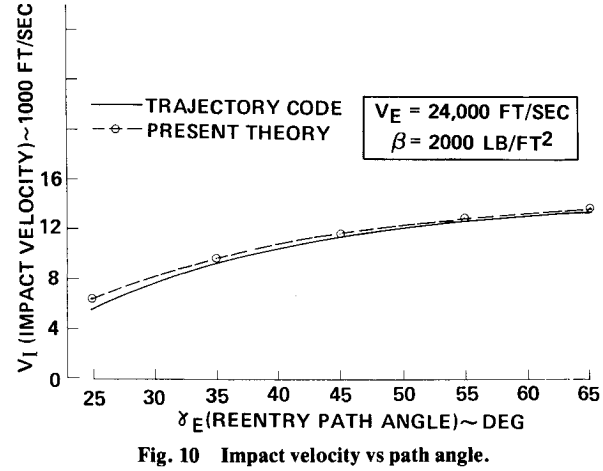

Fig. 10 Impact velocity vs path angle.

and the velocity at the altitude of maximum acceleration is

$$V_4^* = C_5 [(2+m_2)/2]^{-1/m_2} \tag{47}$$

Results

The drag coefficient data for a re-entry vehicle with a cone half-angle of 7 deg and a bluntness ratio of 0.2 are illustrated in Fig. 3. These data were obtained from flowfield code solutions[2] and compare very well with experimental data[3] for a very similar vehicle. Using the appropriate values for the drag constants for this configuration, as obtained from Table 1, the vehicle trajectory was calculated using the theory derived in the previous sections.

The vehicle velocity as a function of altitude is presented in Fig. 6 for a re-entry velocity of 24,000 ft/s and a 25-deg flight path angle. The effect of neglecting the acceleration of gravity is seen primarily at the high altitudes, where the trajectory code indicates a slight velocity increase over the re-entry value. This increase is neglected by the theory. The difference in the velocity at the low altitude is primarily due to the fact that the atmospheric density function does not perfectly match the actual density variation with altitude. The comparison of analytical results with the numerical code results is quite favorable however.

The axial acceleration as a function of altitude is presented in Fig. 7. The theory slightly underpredicts the acceleration before the peak, which results in a shift of the peak to an altitude lower than that calculated by the trajectory code. This is due primarily to the atmospheric density function, which underestimates the density in this region. For example, at the point of peak axial acceleration, the density function underestimates the actual density by 13%. If the theoretical velocity is used with the correct density, the maximum axial

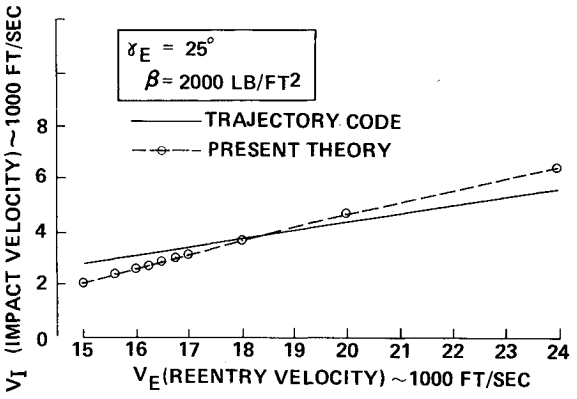

Fig. 11 Impact velocity vs re-entry velocity.

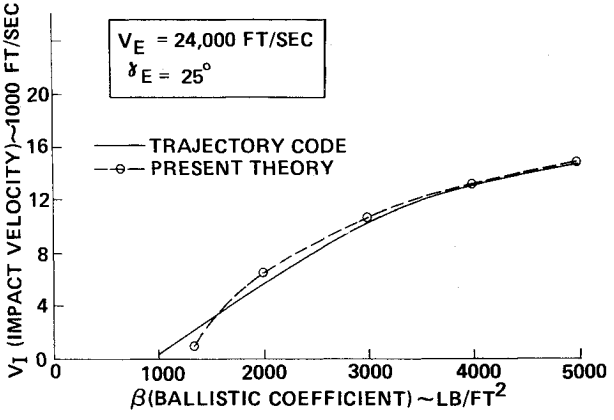

Fig. 12 Impact velocity vs ballistic coefficient.

acceleration is almost exactly the same as the trajectory code value. This suggests that the theoretical values can be considerably improved by this simple adjustment.

The dynamic pressure altitude history is presented in Fig. 8, and it also exhibits a shift of the peak to a lower altitude. The peak value can be similarly improved by using the actual density with the theoretical velocity at this point.

The time to any altitude was not solved in the present paper using variable drag. Using the constant drag relation [Eq. (15)], the analytical altitude history is compared to the trajectory code results in Fig. 9. There is reasonable agreement for this trajectory, but the relation would not be expected to give good results for a wide range of re-entry conditions.

The accuracy of the theory for predicting the impact velocity over a large range of re-entry path angles is illustrated in Fig. 10; the variation of the impact velocity with re-entry velocity is illustrated in Fig. 11. The agreement is good for the parameter range studied; however, at lower velocities, the accuracy rapidly diminishes. The theory should definitely not be used for values of the re-entry velocity which produce impact Mach numbers less than 1, since the two-slope drag function does not model the drag coefficient accurately below $M=1$.

The variation of impact velocity with ballistic coefficient β is presented in Fig. 12. Note that the accuracy drops off rapidly as β decreases below 1500. This is because the impact Mach number is approaching one, and the acceleration of gravity is becoming dominant in the terminal portion of the trajectory.

Conclusions

The present theory has been shown to provide relatively accurate answers for those re-entry conditions and ballistic coefficients that do not result in trajectories that drop below $M=1$ at impact. This limitation is due to the two-slope drag formulation. The accuracy could be improved by going to a three-slope formulation; however, the improvement would not be very significant since the gravity term which was neglected in the derivation can no longer be ignored at these low velocity and acceleration levels.

References

[1] Allen, H.J. and Eggers, A.J., Jr., "A Study of the Motion and Aerodynamic Heating of Ballistic Missiles Entering the Earth's Atmosphere at High Supersonic Speeds," NACA 1381, 1958.

[2] Moretti, G. and Bleich, G., "Three-Dimensional Inviscid Flow About Supersonic Blunt Cones at Angle of Attack," Sandia Laboratories, Albuquerque, N. Mex., SC-CR-68-3728, Sept. 1968.

[3] Barbera, F.J., "Kaman Asymmetric Nosetip Tests, Vol. I, Force and Moment Data," Kaman Sciences Corp., Colorado Springs, Colo., K-79-23U(R), March 20, 1979.